ORGANOMETALLICS

ARTICLE

pubs.acs.org/Organometallics

A New Diphosphite Promoting Highly Regioselective Rhodium-Catalyzed Hydroformylation†

Detlef Selent,*[,‡] Robert Franke,[§] Christoph Kubis,[‡] Anke Spannenberg,[‡] Wolfgang Baumann,[‡] Burkard Kreidler,[§] and Armin Börner*[,‡]

[‡]Leibniz-Institut für Katalyse e. V. an der Universität Rostock, Albert-Einstein-Strasse 29a, D-18059 Rostock, Germany

[§]Evonik Oxeno GmbH, Paul-Baumann-Strasse 1, D-45772 Marl, Germany

Supporting Information

ABSTRACT: A new rhodium catalyst is described that gives 99% regioselectivity in linear aldehyde in the hydroformylation of internal and terminal olefins. High-pressure NMR spectroscopic data verify an energetically preferred bis-equatorial mode of coordination for the bidentate phosphite ligand in the hydride resting state of the catalyst. Experimental FTIR spectra are compared with the individual spectra of the *e,e* and *e,a* isomers of [HRh(CO)$_2$(P∩P)] calculated from density functional theory.

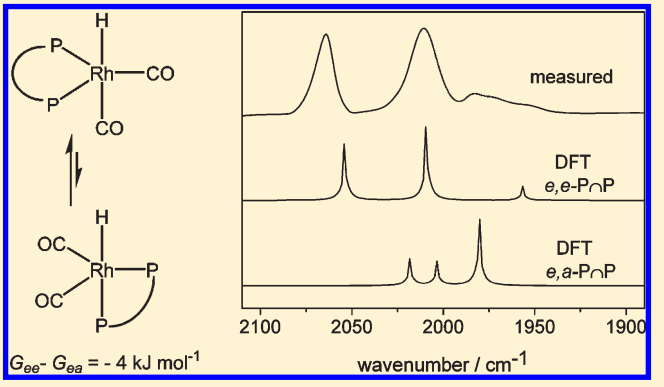

The rhodium-catalyzed hydroformylation of olefins to give aldehydes is an important and widely investigated homogeneously catalyzed reaction.[1] With a terminal olefin used as a substrate, a high molar fraction of *n*-aldehyde is usually desired. This goal can be achieved by choosing rhodium complexes containing rigid bidentate phosphorus ligands which show reduced conformational flexibility. These ligands include diphosphites based on sterically demanding bisphenols.[2] Despite the fact that a large number of diols and (di)phenol derivatives have been used to form diphosphites,[3] the BIPHEPHOS ligand (see Chart 1) is still the most prominent member among them, bearing two seven-membered phosphacycles.[4] With this ligand 98−99% *n*-selectivity is usually seen in terminal olefin hydroformylation. Another advantage is its short and rather cheap synthesis. In contrast, monophosphites induce less regioselectivity, which is usually accompanied by a pronounced substrate double-bond isomerization; the occurrence of this parallel reaction during hydroformylation has been concluded early from the formation of unexpected iso-aldehydes from long-chain olefins.[5,6] Such activity of the catalyst can be of benefit for the production of terminal aldehydes via an isomerization−hydroformylation reaction sequence from internal alkenes, as was shown with rhodium catalysts modified with fluoroalkyl phosphites, diphosphines, and phosphonites.[7] Excellent selectivities to the corresponding *n*-aldehydes from 2-alkenes have recently been obtained with a new, structurally less defined rhodium tetraphosphorus ligand catalyst.[8] With our synthesis of bidentate *O*-acyl phosphites predominant *n*-regioselective catalysts became available, showing very high turnover frequencies (>4000 h^{-1}) for the hydroformylation of internal alkenes.[9,10] For these catalysts, the preference for the *a,e*-[HRh(CO)$_2$(P^1∩P^2)] complex isomer has been confirmed by high-pressure NMR spectroscopy.[11]

Here we will present evidence that very high regioselectivity in both terminal and internal olefin hydroformylation can be achieved when 1,3,2-dioxaphospholane moieties based on a sterically highly demanding substituted 1,2-ethanediol, such as benzpinacol, are part of the ligand structure. Apart from the excellent catalytic performance, the new motif is accessible in a two-step synthesis and has therefore the potential for industrial application.

RESULTS AND DISCUSSION

First, the new ligand building block 2-chloro-4,4′,5,5′-tetraphenyl-1,3,2-dioxaphosphole (**1**) was synthesized, which was easily accessible in nearly quantitative yield from the reaction of benzpinacol with PCl_3 in the presence of triethylamine or *N*,*N*′-dimethylaminobutane in toluene. For details of analyses and the X-ray molecular structure of this compound, see the Supporting Information.

The synthesis of the unsymmetrical ligand **2** involves the reaction of the monolithium salt of 2,2′-dihydroxy-3,3′-di-*tert*-butyl-5,5′-dimethoxybiphenyl with **1** followed by treatment of the hydroxy phosphite intermediate obtained with 2-chloro-1,3,2-benzodioxaphosphorin-4-one in the presence of triethylamine (Scheme 1). Two diastereomers are formed, which are characterized by phosphorus NMR signals centered at 117.0

Received: January 20, 2011
Published: August 15, 2011

(d, J_{PP} = 50.4 Hz), 144.9 ppm (d, J_{PP} = 50.4 Hz) and 118.3 (d, J_{PP} = 51.4 Hz) and 145.3 ppm (d, J_{PP} = 51.4 Hz), respectively, and pronounced spin coupling between the different phosphorus atoms that we interpret in terms of a *through-space* interaction.[12]

For the synthesis of the diphosphites **3** and **4** 2 equiv of the phosphorus chloride **1** was reacted with racemic 1,1′-bi(2-naphthol) or 2,2′-dihydroxy-3,3′-di-*tert*-butyl-5,5′-dimethoxybiphenyl, respectively, leading to an approximately 80% yield after recrystallization. In the ^{31}P NMR spectrum, both compounds exhibit single resonances at 140.5 (**3**) and 145.3 ppm (**4**).

The new ligands were tested in the rhodium-catalyzed hydroformylation of 1-octene and of internal octenes and 2-pentene (Scheme 2). The reaction temperature was set to 120 °C for the internal olefinic substrates to favor olefin isomerization. A comparison with BIPHEPHOS (**5**) is given (see Table 1). It is noteworthy that under the conditions used in this study full chemoselectivity was achieved for all batches.

The diphosphites **2** and **3** form an active rhodium catalyst but do not induce outstanding regioselectivity with 1-octene used as the substrate. For the unsymmetrical **2**, which does contain an anhydridic O-acyl moiety derived from salicylic acid, this is in accord with earlier results obtained for a similar ligand structure.[9] An enhanced reaction rate in the presence of this ligand is reflected in the highest aldehyde yield obtained from internal octenes and 2-pentene, respectively, where the main product is the corresponding *n*-aldehyde (ratio linear:branched 3.2 and 3.9).

Chart 1. Ligands Used in This Study: New Diphosphites 2−4 and 5 (BIPHEPHOS)

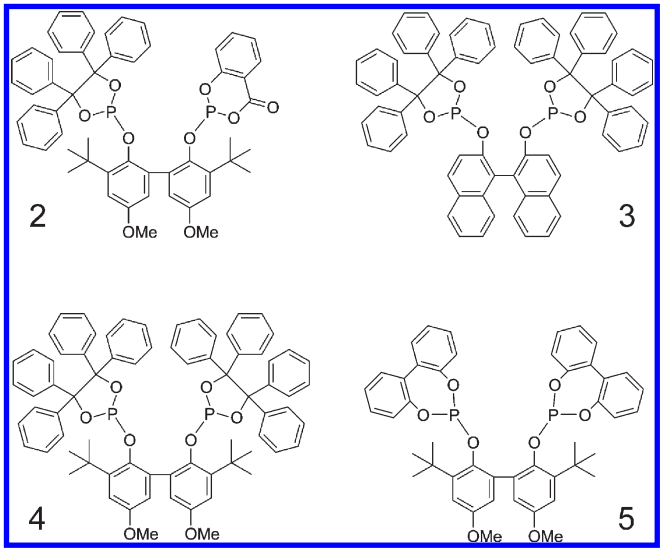

Scheme 2. Parallel and Consecutive Isomerization and Hydroformylation Reactions of 2-Pentene

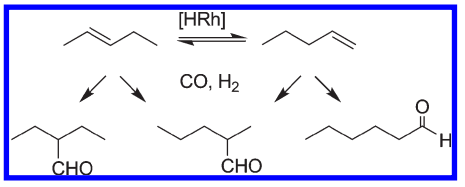

Significantly higher *n*:*iso* product aldehyde ratios were obtained with **4**, even in comparison to the industrial standard BIPHEPHOS. Thus, this ratio is 124 (Rh-**5**: 70.4) from 1-octene and 99 (Rh-**5**: 22) from 2-pentene. The reduced reactivity toward 2-pentene under the standard conditions is obvious and was confirmed by additional experiments. Thus, a doubled concentration of the Rh-**4** catalyst together with a prolonged reaction time of 24 h was needed to enhance the yield of hexanals from 14% to 63%. This was accompanied by a small drop in *n*-selectivity from 99.0 to 97.5%. When the ligand **4** to Rh ratio was increased from 2 to 5, no effect on hexanal yield and regioselectivity could be observed.

Interestingly, the Rh-**5** catalyst from the literature worked similarly with the different internal olefins. Thus, 93.3% *n*-nonanal from the octene mixture and 95.8% *n*-hexanal from 2-pentene were obtained. This points to a similar balanced kinetic control between olefin isomerization and terminal and internal hydroformylation for both substrates. With Rh-**4**, the selectivity obtained from the octenes is only ∼70% but a higher aldehyde yield was obtained compared to 2-pentene with the first-order rate constant k_{obs} = 1.8 × 10^{-3} min^{-1}. A time-dependent plot of the molar fractions of the octane isomers shows that after an initial period of 50 min with ongoing hydroformylation the ratio of the individual isomers remains constant (see Figure 1). The 0.01 fraction determined for 1-octene fits to the thermodynamic equilibrium value.[13] The fraction of 2-octene (cis + trans) is depleted to 0.38 (equilibrium: 0.45), whereas the 3- and 4-octenes are populated to 0.36 (0.32) and 0.24 (0.22). 2-Octene, therefore, is more reactive in hydroformylation than the other internal isomers and isomerization is not fast enough to equilibrate the octenes. Consequently, the initial change of olefin composition is accompanied by a decrease of *n*-nonanal selectivity.

Hydroformylation of 2-pentene proceeds with the first-order rate constant k_{obs} = 7.2 × 10^{-4} min^{-1}. The composition of the substrate mixture changes continuously with the less reactive trans isomer, accumulating to a 0.78 mol fraction after 4 h.[14] This is significantly above the equilibrium value of 0.69 (see

Scheme 1. Ligand Synthesis, Exemplified for the Unsymmetrical Diphosphite 2

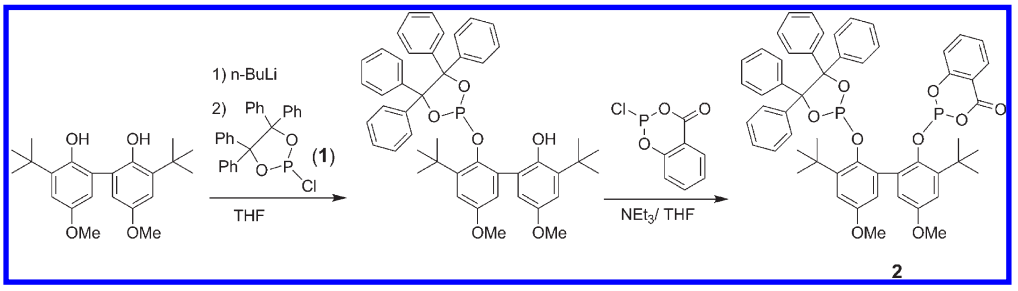

dx.doi.org/10.1021/om2000508 |*Organometallics* 2011, 30, 4509–4514

Table 1. Hydroformylation[a] of 1-Octene,[b] *n*-Octenes,[c,d], and 2-Pentene[c]

	yield of nonanal (%)/ *n*-selectivity (%)		yield of hexanal (%)/ *n*-selectivity (%)
ligand	1-octene	*n*-octenes[e]	2-pentene[f]
2	87/92.9	88/76.2	98/79.8
3	93/87.5	28/72.2	83/63.6
4	90/99.2	39/69.8	14/99.0[g]
5	92/98.6	50/93.3	83/95.8

[a] Conditions: solvent toluene, ligand to rhodium ratio 2, t = 4 h. [b] Conditions: T = 100 °C, p = 50 bar, precursor [acacRh(CO)$_2$], [Rh] = 0.3 × 10^{-3} M. [c] Conditions: T = 120 °C, p = 20 bar (constant), [Rh] = 0.75 × 10^{-3} M. [d] A technical internal octene mixture was used; see the Supporting Information. [e] [octenes] = 1.62 M. [f] [2-pentene] = 2.35 M. [g] The same result was obtained with a ratio **4**/Rh= 5.

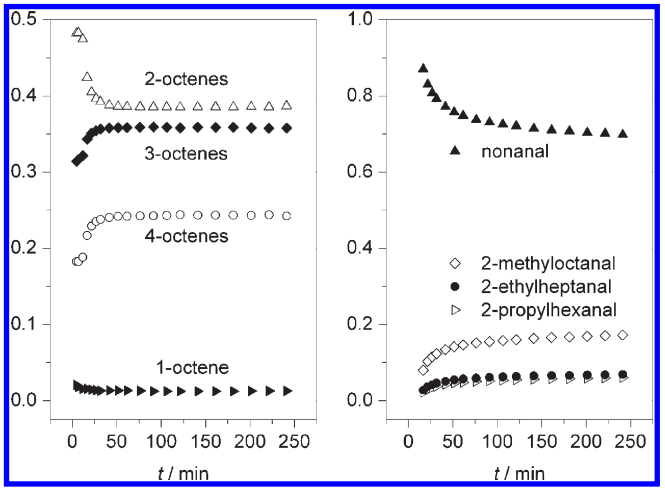

Figure 1. Isomerization/hydroformylation of internal octenes with the Rh-**4** catalyst: time-resolved plot of molar fractions of octenes (left; initial fraction of 1-octene was 0.03) and C_9 aldehyde isomers (right). For the reaction conditions, see Table 1.

Figure 2).[13] Similar to the the case for the octenes, the terminal isomer constantly levels at 0.01 (equilibrium: 0.03). The time-resolved in situ FTIR spectra taken during the reaction prove the stability of the catalyst and the presence of [HRh(CO)$_2$(**4**)] as the only resting state over the full reaction period, a result which was also verified for the hydroformylation of internal octenes.

The low 1-pentene concentration observed during catalysis, together with the high product regioselectivity obtained, proves that the *n*-aldehyde is formed in a consecutive reaction. The major reaction pathway includes *cis*-2-pentene, which is depopulated. Furthermore, the high regioselectivity observed points to a strong tendency of the isopentyl intermediates to hydride elimination and 1-pentene complex formation.[15,16] Such a double-bond shift could proceed even faster with the octenes, because a chain length dependency in olefin isomerization has recently been rationalized for rhodium diphosphine catalysts.[17] The lower regioselectivity obtained with the internal octene hydroformylation needs further explanation, and a detailed kinetic analysis of both reactions, isomerization and hydroformylation, is required, as has been exemplified for the *n*-dodecene isomers.[18]

The formation of the most efficient hydroformylation catalyst, Rh-**4**, was studied by high-pressure NMR spectroscopy under conditions comparable to those for the catalytic batch routine. Thus, the catalyst precursor [acacRh(CO)$_2$] was treated with **4** in toluene-d_8 under an argon atmosphere and the resulting solution was then transferred to a modified 10 mm high-pressure sapphire NMR tube. With the sample placed inside the magnet, a mixture of CO and H_2 (1:1) was supplied to the reaction solution via capillary at a constant head space pressure of 20 bar. This was done for the whole time of the experiment to ensure gas saturation. After heating to 70 °C, the reaction mixture equilibrated within 30 min.

The spectroscopic data obtained confirm the clean formation of the rhodium hydride [HRh(CO)$_2$(**4**)] (see Scheme 3) together with equimolar amounts of acetylacetone. The hydrido complex is characterized by a proton resonance at −10.00 ppm (d, J_{HRh} = 3.4 Hz) and a broadened phosphorus signal at 166.1 ppm (d, J_{PRh}= 235 Hz). The lack of any observable H−P coupling and the equivalency of both phosphorus nuclei point to a preference for *e,e* coordination of the diphosphite, with the hydride located in an axial position. The spectrum of the hydride remained unchanged upon cooling to room temperature and depressurization. IR measurement of the syngas-saturated NMR sample resulted in bands at $\tilde{\nu}$(CO) 1985 (w), 2012 (vs) and 2065 (vs) cm^{-1} (trace A in Figure 4), equal to that observed during hydroformylation. This agrees with the observation of equivalent phosphorus atoms by NMR spectroscopy, since two absorptions around 2020 and 2070 cm^{-1} are indicative of the bis-equatorial ligand coordination.[19] The resonance at 1985 cm^{-1} can be assigned to *e,a*-[HRh(CO)$_2$(**4**)]. It is noteworthy that NMR spectroscopy cannot differentiate between the two hydride isomers at ambient temperature, although the broadened phosphorus signal might be due to the respective rotational dynamics. In order to confirm these results, we also performed quantum chemical DFT calculations for each of the isomeric *e,a* and *e,e* rhodium hydride complexes (see Figure 3 for *e,e*- and *e,a*-[HRh(CO)$_2$(**4**)]). These calculations verify a stabilization by 4 kJ/mol for the latter isomer at 298 K, which predominates with a content of 80% in the isomer mixture at room temperature. For the calculated structures, see Figure 3. With an P−Rh−P angle of 120.7° the *e,e* isomer approaches the idealized tbp geometry.

In Figure 4 the overlapping experimental FTIR spectrum is compared with the theoretical spectra obtained for the individual rhodium hydride complexes. The calculation shows that all absorptions of the HRh(CO)$_2$ fragments within the range from 1900 to 2100 cm^{-1} arise from a simultaneous excitation of Rh−H and CO stretching vibrations. Despite some frequency shift, the calculated spectra fit relatively well to the experiment with strong absorptions at 2010 and 2054 cm^{-1} and the relative band intensities obtained for the *e,e* and the band for the *e,a* isomer located at 1981 cm^{-1}. The weak absorptions at 2004 and 2019 cm^{-1} calculated for the latter isomer are not resolved experimentally, owing to overlap and the relatively low molar fraction of this complex.

Isolable rhodium complexes of ligand **4** have been easily obtained at room temperature in toluene by substitution of the neutral ligands from [(acac)Rh(CO)$_2$] and [(η^3-C_3H_5)Rh(COD-1.5)] with 1 equiv of diphosphite to yield [(acac)Rh(**4**)][21] and [(η^3-C_3H_5)Rh(**4**)], respectively. The solution NMR spectroscopic data of the latter complex are consistent with

dx.doi.org/10.1021/om2000508 |*Organometallics* 2011, 30, 4509–4514

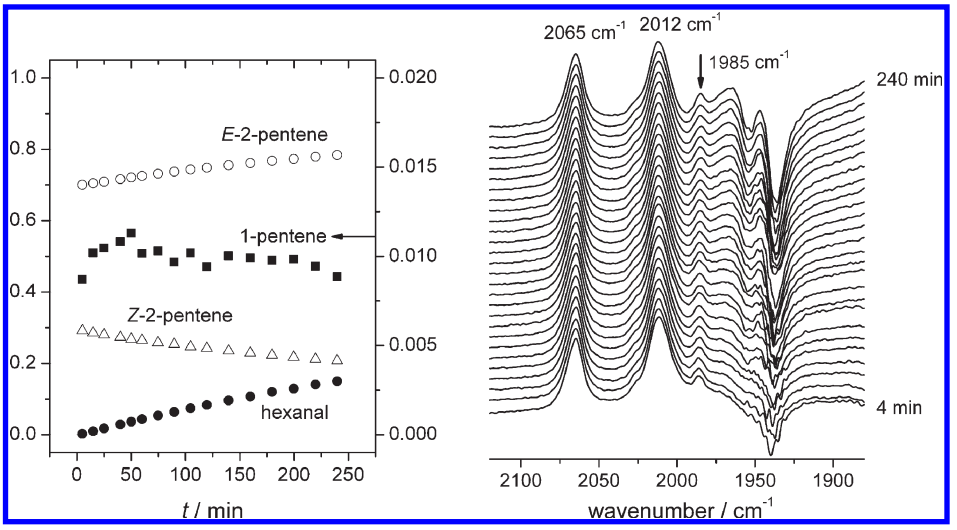

Figure 2. Isomerization/hydroformylation of (*E*)-/(*Z*)-2-pentene with the Rh-**4** catalyst. (left) Yield versus time of hexanal (×100%) and profiles of molar fractions of 2-pentenes (main axis) and of 1-pentene (secondary axis). The final mole fraction of *cis*-2-pentene is 0.21 (equilibrium: 0.28); for further details see text). (right) In situ FTIR spectra of the metal carbonyl region (alterations of the baseline from 1925 to 1975 cm^{-1} are due to background subtraction). Reaction conditions: T = 120 °C, p = 20 bar ($CO:H_2$ = 1:1), t = 4 h, solvent toluene.

Scheme 3. Formation of *e,e*-[$HRh(CO)_2$(4**)]**

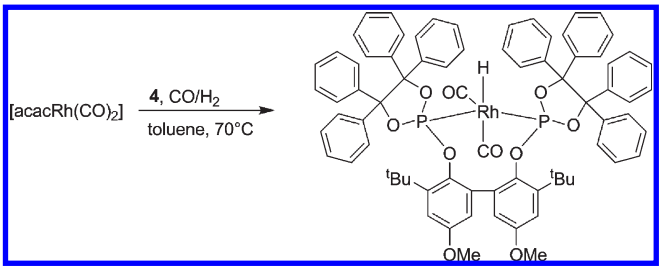

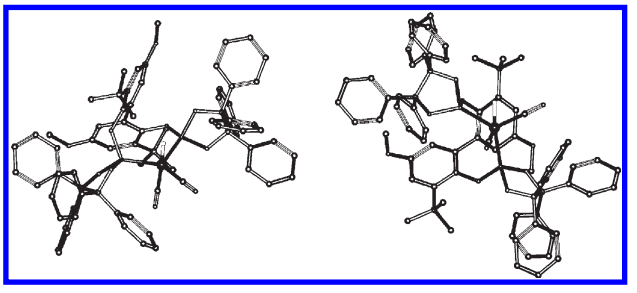

Figure 3. Structures from DFT calculations[20] of (left) *e,e*- and (right) *e,a*-[$HRh(CO)_2$(**4**)]. The angles P−Rh−P are 120.7° for the *e,e* and 110.3° for the *e,a* isomer. Rh−P bond lengths for the *e,e* isomer are respectively 2.33 and 2.29 Å and for the *e,a* isomer are 2.34 Å (*a*-P) and 2.37 Å (*e*-P).

a rigid and unsymmetrical η^3 bonding mode of the allyl ligand. Each of the allyl H_{syn} and H_{anti} protons is separately detectable, as in [(η^3-2-Me-C_3H_5)Rh(arphos)].[22] Resonances centered at 1.97 (t, $^3J_{HP}$ = 11.7 Hz; H_{a1}), 2.53 (dd, $^3J_{HP}$ = 13.1 Hz, $^3J_{HP}$ = 9.9 Hz; H_{a2}), 3.08 (m, H_{s1}), 3.79 (m, H_{s2}) and 4.69 ppm (m, H_m) are observed. Due to slow intermolecular movement, including hindered allyl group rotation, an extra data set is observed not only for the substructures of the ligand backbone but also the phosphorus atoms, which resonate at 166.4 (dd, J_{PRh} = 326.0 Hz,

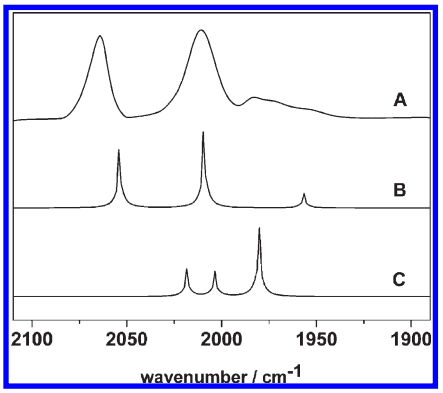

Figure 4. FTIR absorption spectra: (A) room-temperature experimental spectrum of [$HRh(CO)_2$(**4**)] (CaF_2, 0.1 mm) after toluene-d_8 solvent spectrum subtraction; (B, C) spectra from DFT theoretical calculations (298 K) of *e,e*-[$HRh(CO)_2$(**4**)] (B) and *e,a*-[$HRh(CO)_2$(**4**)] (C).[20]

$^2J_{PP}$ = 58.5 Hz) and 169.1 ppm (dd, J_{PRh} = 320.1 Hz, $^2J_{PP}$ = 58.5 Hz). The coupling constants J_{PRh} are considerably higher than those measured for corresponding rhodium complexes with bidentate phosphines (169−200 Hz) and are in the same range of the values of 317 and 304 Hz found for the allyl-type diphosphite complex *syn*-[(η^3-2,4-dimethylpentadienyl)Rh(pinacop)].[23,24]

In the molecular structure (Figure 5) a distorted-planar coordination at rhodium can be observed, with the allyl group occupying two cis positions at the rhodium atom and with a mean deviation of 0.08 Å from the best plane through Rh, P1, P2, C1, and C3. The P1−Rh1−P2 angle is 104.49(2)°, which points to the flexibility of the ligand as compared with the angle of 120.7° calculated for *e,e*-[$HRh(CO)_2$(**4**)] and is just midway between the ideal values of 120° for bis-equatorial (*e,e*) and 90 °C for equatorial−axial (*e,a*) diphosphite coordination in tbp-structured hydrides [$HRh(CO)_2$(P∩P)].[25] In contrast, the reduced steric demand present in the bis(triphenyl phosphite) complex (η^3-C_3H_5)Rh[$P(OPh)_3$]$_2$ results in a P−Rh−P angle of 97.55° and shorter P−Rh bonds.[26] The structure of [(η^3-C_3H_5)Rh(**4**)]

dx.doi.org/10.1021/om2000508 |*Organometallics* 2011, 30, 4509–4514

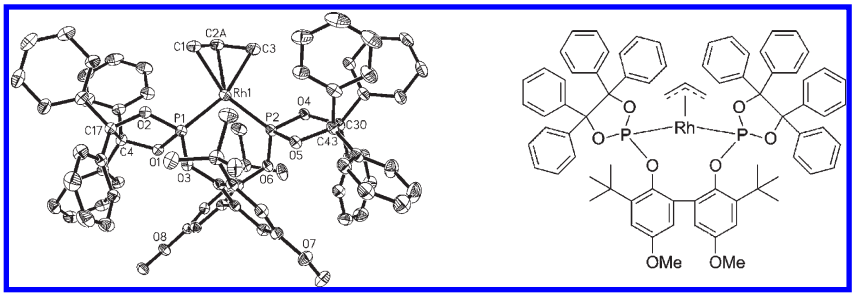

Figure 5. Molecular structure of $[(\eta^3\text{-}C_3H_5)Rh(\mathbf{4})]$. Thermal ellipsoids represent 30% probability. Hydrogen atoms are omitted. Selected geometric data: P1−Rh1 = 2.2016(6) Å, P2−Rh1 = 2.2039(6) Å, P1−Rh1−P2 = 104.49(2)°, C1−Rh1 = 2.176(2) Å, C3−Rh1 = 2.177(2) Å, C1−C2A−C3 = 115.5(3)°.

also proves the capability of the phosphorus ligand of providing a pocketlike environment for the rhodium center. Such a crowded ligand arrangement has been discussed to be essential for the relatively high *n*:*iso* product ratio of 46 that is observed in the propene hydroformylation promoted by (*S*,*R*,*S*)-6,6′-$(CH_3)_2$-BIPHEPHOS.[27]

CONCLUSION

A benzpinacol substructure was included into a bisphosphite ligand used in Rh-catalyzed hydroformylation. This motif reduces the activity of the catalyst toward the undesired hydroformylation of internal olefins. As a consequence, with 1-octene an outstandingly high l:b aldehyde ratio of 124 is achieved. Remarkable regioselectivity is also obtained in the consecutive isomerization−hydroformylation of 2-pentene. Regioselectivity and activity are significantly influenced by the chain length of the olefinic substrate. The spectroscopic and theoretical results obtained for the Rh-**4** catalytic system are in accord with previous experience that, for highly regioselective catalysts, bis-equatorial diphosphite coordination is typical for the resting state of the catalyst. Due to the straightforward synthesis of the new ligand, it has the potential of broad application in academic and industrial hydroformylation. The first evidence was already given by Haumann and Wasserscheid, who used the ligand in supported ionic liquid phase (SILP) catalysis for the highly selective hydroformylation of mixed C4 feedstocks.[28]

ASSOCIATED CONTENT

Supporting Information. Text, tables, figures, and CIF files giving experimental procedures, compound characterization data, crystallographic data for compounds **1** and $[(\eta^3\text{-}C_3H_5)Rh(\mathbf{4})]$, details on DFT quantum calculations, and an overlap of the experimental structure with the quantum chemically calculated structure of $[\eta^3\text{-}C_3H_5Rh(\mathbf{4})]$. This material is available free of charge via the Internet at http://pubs.acs.org.

AUTHOR INFORMATION

Corresponding Authors

*D.S.: tel, ++49-381-1281169; fax, ++49-381-128151169; e-mail, detlef.selent@catalysis.de. A.B.: email, armin.boerner@catalysis.de.

ACKNOWLEDGMENT

We appreciate financial support from Evonik Oxeno GmbH, Marl, Germany. Support from Dr. D. Hess (Evonik Oxeno GmbH) and Dr. B. Hannebauer (AQura GmbH, Evonik Industries) regarding FTIR spectroscopy and DFT quantum chemical calculations is gratefully acknowledged.

DEDICATION

†Dedicated to Professor Rudolf Taube on the occasion of his 80th birthday.

REFERENCES

(1) (a) *Rhodium Catalyzed Hydroformylation*; van Leeuwen, P. W. N. M., Claver, C., Eds.; Kluwer: Dordrecht, The Netherlands, 2000. (b) Protzmann, G.; Wiese, K.-D. *Erdöl, Erdgas, Kohle* **2001**, *117*, 235-240. (c) Wiese, K.-D., Obst, D. Hydroformylation. In *Catalytic Carbonylation Reactions*; Beller, M., Ed.; Springer: Heidelberg, Germany, 2008; Topics in Organometallic Chemistry 18, p 1.

(2) Billig, E.; Abatjoglou, A. G.; Bryant, D. R. US 4668651, 1987 and US 4769498, 1988 (UCC).

(3) Urata, H.; Itagaki, H.; Takahashi, E.; Wada, Y.; Tanaka, Y.; Ogino, Y. U.S. Patent 5 910 600, 1997 (Mitsubishi Chem. Corp.).

(4) (a) Cuny, G. D.; Buchwald, S. L. *J. Am. Chem. Soc.* **1993**, *115*, 2066. (b) Moasser, B.; Gladfelter, W. L.; Roe, D. C. *Organometallics* **1995**, *14*, 3832. (c) van Rooy, A.; Kamer, P. C. J.; van Leeuwen, P. W. N. M. *J. Organomet. Chem.* **1997**, 201. (d) Rush, S. N.; Noskov, Y. G.; Kron, T. E.; Korneeva, G. A. *Kinet. Catal.* **2009**, 557.

(5) (a) van Rooy, A.; De Bruijn, J. N. H.; Roobeek, K. F.; Kamer, P. C. J.; van Leeuwen, P. W. N. M. *J. Organomet. Chem.* **1996**, *507*, 69. (b) van Rooy, A.; Kamer, P. C. J.; van Leeuwen, P. W. N. M.; Goubitz, K.; Fraanje, J.; Veldman, N.; Spek, A. L. *Organometallics* **1996**, *15*, 835.

(6) (a) Asinger, F.; Berg, O. *Chem. Ber.* **1955**, *88*, 445. (b) Keulemans, A. J. M.; Kwantes, A.; van Bavel, T. *Recl. Trav. Chim. Pays-Bas* **1948**, *67*, 298.

(7) (a) van Leeuwen, P. W. N. M.; Roobeek, K. F. Brit. Patent 2 068 377, 1980 (Shell). (b) van der Veen, L. A.; Kamer, P. C. J.; van Leeuwen, P. W. N. M. *Angew. Chem., Int. Ed.* **1999**, *38*, 336. (c) van der Veen, L. A.; Kamer, P. C. J.; van Leeuwen, P. W. N. M. *Organometallics* **1999**, *18*, 4765. (d) Klein, H.; Jackstell, R.; Wiese, K.-D.; Borgmann, C.; Beller, M. *Angew. Chem., Int. Ed.* **2001**, *40*, 3408. (e) Selent, D.; Wiese, K.-D.; Röttger, D.; Börner, A. *Angew. Chem., Int. Ed.* **2000**, *39*, 1639. (f) Seayad, A.; Ahmed, M.; Klein, H.; Jackstell, R.; Gross, T.; Beller, M. *Science* **2002**, *297*, 1676.

(8) (a) Yan, Y.; Zhang, X.; Zhang, X. *J. Am. Chem. Soc.* **2006**, *128*, 16058. (b) Yu, S.; Chie, Y.; Guan, Z.; Zhang, X. *Org. Lett.* **2008**, *10*, 3469.

(9) Selent, D.; Hess, D.; Wiese, K.-D.; Röttger, D.; Kunze, C.; Börner, A. *Angew. Chem., Int. Ed.* **2001**, *40*, 1696.

(10) An enhanced olefin isomerization rate due to the reduced σ-donor character of the O-acyl phosphite moiety is probable. A similar effect was observed earlier in olefin hydrogenation with catalysts containing less donating ligands: Schrock, R. R.; Osborn, J. A. *J. Am. Chem. Soc.* **1976**, *98*, 2134.

(11) Selent, D.; Wiese, K.-D.; Börner, A. In *Catalysis of Organic Reactions*; Sowa, J. R., Ed.; Taylor & Francis: Boca Raton, FL, 2005; Vol. 20, p 459.

(12) (a) Diz, A. C.; Contreras, R. H.; Natiello, M. A.; Gavarini, H. O. *J. Comput. Chem.* **1985**, *6*, 647. (b) Perera, D.; Shaw, B. L.; Thornton-Pett, M.; Vessey, J. D. *Inorg. Chim. Acta* **1993**, 175. (c) Hierso, J.-C.; Fihri, A.; Ivanov, V. V.; Hanquet, B.; Pirio, N.; Donnadieu, B.; Rebière, B.; Amardeil, R.; Meunier, P. *J. Am. Chem. Soc.* **2004**, *126*, 11077. (d) Hierso, J.-C.; Evrard, D.; Lucas, D.; Richard, P.; Cattey, H.; Hanquet, B.; Meunier, P. *J. Organomet. Chem.* **2008**, *693*, 574.

(13) Alberty, R. A.; Gehrig, C. A. *J. Phys. Chem. Ref. Data* **1985**, *14*, 803.

(14) This is similar to the reactivity of unsaturated fatty acid derivates: Muilwijk, K. F.; Kamer, P. C. J.; van Leeuwen, P. W. N. M. *J. Am. Oil Chem. Soc.* **1997**, *74*, 223.

(15) Casey, C. P.; Petrovich, L. M. *J. Am. Chem. Soc.* **1995**, *117*, 6007.

(16) With rhodium, it is accepted that olefin isomerization takes place via the hydride migration−elimination route, which can occur parallel to hydroformylation, leading to isomerized substrate in the reaction mixture: Cramer, R. *J. Am. Chem. Soc.* **1966**, *88*, 2272. Stefani, A.; Consiglio, G.; Botteghi, C.; Pino, P. *J. Am. Chem. Soc.* **1977**, *99*, 1058.

(17) Carvajal, M. À.; Kozuch, S.; Shaik, S. *Organometallics* **2009**, *28*, 3656.

(18) (a) Cornely, W. Ph.D. Thesis, RWTH Aachen, Aachen, Germany, 1979. (b) Cornely, W.; Fell, B. *Chem. Z.* **1981**, *105*, 317. Frankel, E. N. *J. Am. Oil Chem. Soc.* **1971**, *48*, 248.

(19) (a) van Rooy, A.; Kamer, P. C. J.; van Leeuwen, P. W. N. M.; Goubitz, K.; Fraanje, J.; Veldman, N.; Spek, A. L. *Organometallics* **1996**, *15*, 835. (b) Buisman, G. J. H.; van der Veen, L. A.; Klootwijk, A.; de Lange, W. G. J.; Kamer, P. C. J.; van Leeuwen, P. W. N. M.; Vogt, D. *Organometallics* **1997**, *16*, 2929. (c) Castellanos-Páez, A.; Castillón, S.; Claver, C.; van Leeuwen, P. W. N. M.; de Lange, W. G. J. *Organometallics* **1998**, *17*, 2543. (d) Buisman, G. J. H.; van der Veen, L. A.; Kamer, P. C. J.; van Leeuwen, P. W. N. M. *Organometallics* **1997**, *16*, 5681. (e) Buisman, G. J. H; Vos, E. J.; Kamer, P. C. J.; van Leeuwen, P. W. N. M. *J. Chem. Soc., Dalton Trans.* **1995**, 409.

(20) The DFT calculations were performed with the TURBOMOLE suite of programs using the functional BP86 employing the RI-*J* approximation and, for all atoms except Rh, a valence double-ζ basis including one set of polarization functions (SVP). The basis set for Rh was a slightly modified valence basis set together with an effective core potential replacing 28 core electrons up to 3d. For more details see the Supporting Information.

(21) For details of synthesis and characterization, see the Supporting Information.

(22) Fryzuk, M. *Inorg. Chem.* **1982**, *21*, 2134.

(23) Manger, M.; Wolf, J.; Teichert, M.; Stalke, D.; Werner, H. *Organometallics* **1998**, *17*, 3210.

(24) Bleeke, J. R.; Donaldson, A. J.; Peng, W.-J. *Organometallics* **1988**, *7*, 33.

(25) For a graphical overlap of the X-ray and calculated structures of $[(\eta^3\text{-}C_3H_5)Rh(\mathbf{4})]$ as well as details of DFT quantum chemical calculations, see the Supporting Information.

(26) John, K. D.; Salazar, K. V.; Baker, R. T.; Sattelberger, A. P. Private communication to the Cambridge Structural Database, deposition number CCDC 147142, 2001.

(27) Briggs, J. R.; Whiteker, G. T. *Chem. Commun.* **2001**, 2174.

(28) Jakuttis, M.; Schönweiz, A.; Werner, S.; Franke, R.; Wiese, K. D.; Haumann, M.; Wasserscheid, P. *Angew. Chem., Int. Ed.* **2011**, *50*, 4492.